THE ASTROPHYSICAL JOURNAL, 437:449–457, 1994 December 10

IRON LINE INTENSITY VARIATIONS OF HERCULES X-1 OVER THE PULSE PHASE AND THE 35 DAY CYCLE

C. S. CHOI,[1] F. NAGASE,[2] F. MAKINO,[2] T. DOTANI,[2] S. KITAMOTO,[3] AND S. TAKAHAMA[3]
Received 1993 November 17; accepted 1994 June 16

ABSTRACT

We have studied the iron line intensity variation of Her X-1 over its characteristic periodicities such as the pulse period of 1.24 s, the orbital period of 1.7 days, and the long-term period of 35 days, with *Ginga* observations made from 1989 April to June. From an analysis of the pulse phase-resolved spectra obtained from the MAIN HIGH state of Her X-1, we discover that the line flux modulates from $(4.3 \pm 1.9) \times 10^{-3}$ to $(1.0 \pm 0.3) \times 10^{-2}$ photons cm^{-2} s^{-1} (the average 7.5×10^{-3} cm^{-2} s^{-1}) during the pulse period. We also find that the line flux modulation is consistent with that of soft X-rays below 1 keV observed by previous authors. From the study of the orbital phase and the 35 day cycle dependences, we see the following facts: (1) the line flux observed during the high intensity state of Her X-1 does not depend significantly on the orbital phase of 0.2–0.9, while the flux is almost invisible during the eclipse, (2) the pattern of the iron line flux modulation along the 35 day cycle is very similar to that of the continuum X-ray flux. With the line pulsations and the solid angle required to explain the equivalent width of the line in the MAIN HIGH state, we deduce that the extent of reprocessing site is less than 10^{10} cm. Based on the similarity of the modulation pattern between the line flux and the continuum flux along the 35 day cycle, and the equivalent width change, we suggest that the line flux variation is mainly due to occultation of the reprocessing site by an accretion disk rather than to a change of reprocessing site; some line flux, very small compared with the MAIN HIGH line flux, from an additional site may be responsible for the equivalent width change.

Subject headings: binaries: eclipsing — pulsars: individual (Hercules X-1) — stars: individual (Hercules X-1) — X-rays: stars

1. INTRODUCTION

Iron emission lines, centered at around 6.4 keV, have been observed in the spectra of most X-ray pulsars (White, Swank, & Holt 1983; Nagase 1989). The general understanding of the line is that it is produced from ions less ionized than Fe XVIII in a relatively cool circumstellar matter by fluorescent Kα transition. In low-mass X-ray binaries, a 6.7 keV iron line is prominent (White et al. 1986; Hirano et al. 1987).

A correlation between the iron line flux and the continuum intensity of 7.1–30 keV was revealed for several binary X-ray pulsars such as Vela X-1 (Ohashi et al. 1984b) and GX 301−2 (Leahy et al. 1989). Moreover, the line intensity modulations as a function of the orbital phase for Vela X-1 (Nagase et al. 1986; Sato et al. 1986) and over the pulse phase for GX 301−2 (Leahy & Matsuoka 1990) have also been detected. The intensity variations have been interpreted as due to obscuration of the line emission site by the companion star (during the eclipse), or to asymmetry in the gas distribution around the neutron star rather than to be the intrinsic variation in the continuum X-ray intensity. Pulsed iron line emission, which exhibits a phase difference, has most recently been discovered from Cen X-3 by Day et al. (1993).

With respect to Her X-1, which is an eclipsing binary X-ray pulsar with a pulse period of 1.24 s and an orbital period of 1.7 days as well as a quasi-periodic X-ray intensity variation of 35 days (Tananbaum et al. 1972; Giacconi et al. 1973), the line feature at ~6.4 keV was discovered by Pravdo et al. (1977a, 1978) from spectra of a high- and low-intensity states of the 35 day cycle. The 6.4 keV iron line was identified by the observation with the gas scintillation proportional counters aboard *Tenma* and *EXOSAT* (Ohashi et al. 1984a; Gottwald & White 1990). Kahabka et al. (1985) have reported that the iron line of Her X-1 is present during all phases of the 35 day cycle. Mihara et al. (1991) suggested a co-existence of 6.4 and 6.7 keV lines from recent *Ginga* observation of the low-state of Her X-1. From detailed spectroscopic study of the pre-eclipse dip of Her X-1, Choi et al. (1994b) found a correlation between hydrogen column density of a material obscuring the line of sight and the line intensity. Iron lines observed in the Her X-1 spectra exhibit the following features; (1) the line center energy is at around 6.4 keV, (2) the line width is ~1 keV (FWHM), (3) the equivalent width changes from 0.2 keV (MAIN HIGH state) to ~1 keV (low state), and (4) the line intensity of the low-intensity state is about one-tenth of that of the MAIN HIGH state.

For the reprocessing site of the iron line of Her X-1, the following sites have been suspected: a vertically extended outer edge of an accretion disk, atmosphere of the companion star, an accretion disk corona, and an Alfvén surface where the accretion flow is distorted and compelled to spread out vertically to the disk plane (see Basko & Sunyaev 1976; Ghosh & Lamb 1979). Among these, however, the companion star atmosphere has been ruled out as a major line emission site, because the expected solid angle subtended at the neutron star is too small to explain the observed equivalent width of ~0.2 keV during the MAIN HIGH state (Pravdo et al. 1977a; Basko 1978, 1980; Bai 1980b). In relation to the suggestions that the origin is disk edge (Bai 1980a; Mihara et al. 1991) or the Alfvén surface (Pravdo et al. 1977a; Basko 1980; Bai 1980b), it is

[1] Korea Astronomy Observatory, 36-1 Whaam-dong Taejeon 305-348, Korea; cschoi@hanul.issa.re.kr.
[2] The Institute of Space and Astronautical Science, 1-1 Yoshinodai 3-chome, Sagamihara, Kanagawa 229, Japan; nagase@astro.isas.ac.jp.
[3] Department of Earth and Space Sciences, Faculty of Science, Osaka University, 1-1 Machikaneyama-cho, Toyonaka, Osaka 560, Japan; kitamoto@oskar.kek.ac.jp.

pointed that the difference may be due to the data sets they included. For instance, the accretion disk edge suggestion is based on the low-state observations, whereas the Alfvén surface region has been proposed from the MAIN HIGH observations.

The typical line intensity of the low-state is ~10% of that of the MAIN HIGH. Two possibilities could be considered on the line-intensity change. The first one is due to change of the line-emission site with the phase of 35 day cycle. The other one is due to occultation of the emission site by the accretion disk like that the continuum X-ray variations. To examine such possibilities, this study is concerned about the line intensity variation, together with the equivalent width change, along the 35 day cycle. In addition, a line intensity modulation over the pulse phase is studied.

2. OBSERVATIONS

Ginga observed Her X-1 16 times during the period of from 1989 April 26 to June 9 (see Deeter et al. 1994). Those observations were made with the Large Area Counter (LAC) which consists of eight proportional counter modules with a total effective area of 4000 cm^2 (Makino et al. 1987), and were mostly allocated to the high-intensity states of Her X-1 (e.g., the MAIN HIGH and the SHORT HIGH state). The LAC covers an energy range of 1–37 keV and has an energy resolution of 18.0% at 6 keV (Turner et al. 1989). Among the observations, we sample the data made with the MPC-2 high bit-rate mode (48 energy channels at 62.5 ms time resolution), which is listed in Table 1. The high intensity of the selected data sets from April 27 to May 4 in the table indicate that the observation period corresponds to a MAIN HIGH state among the characteristic intensity states of the 35 day cycle. We also use a low-state spectrum presented by Mihara et al. (1991), as well as an eclipse spectrum obtained by Choi et al. (1994a), to understand the iron line intensity variation over the various continuum X-ray levels of Her X-1.

In order to search for a pulse-phase dependence of the line, phase-resolved spectra are made with ephemeris and pulse period determined by Deeter et al. (1991), in which the data observed from April 27 to May 4 in 1989 have been accumulated. Using those data sets we obtain a phase-averaged pulse profile shown in Figure 1. Background was subtracted using the blank sky observation of nearby Her X-1 ($\alpha = 246°$, $\delta = 44°$). The pulse is divided into 20 phases, and the spectrum corresponding to each phase is analyzed in the following section. For the SHORT HIGH state, however, we could not make the phase-resolved spectrum have enough statistics because of insufficient data made with MPC-2 mode during the period. Hence we restrict our study on the pulse-phase dependence to the MAIN HIGH state.

TABLE 1

THE HERCULES X-1 OBSERVATIONS WITH *Ginga* LARGE AREA COUNTER

START (1989)		END (1989)				
	(hr:minutes)		(hr:minutes)	Φ_{orb}[a]	Ψ_{35}[a]	FLUX[b]
Apr 27	20:45	Apr 27	20:51	0.22	0.04	1284.5
Apr 30	17:42	Apr 30	17:50	0.91	0.12	1342.9
May 1	20:39	May 1	20:49	0.57	0.15	1266.1
May 3	15:31	May 3	15:37	0.62	0.20	875.8
May 4	15:30	May 4	15:36	0.20	0.23	590.1
May 18	11:42	May 18	11:52	0.35	0.63	352.5
May 20	10:01	May 20	10:06	0.48	0.68	275.9

[a] The epoch from Deeter et al. 1991.
[b] The energy range is 1.7–37 keV and the units are in counts s^{-1}.

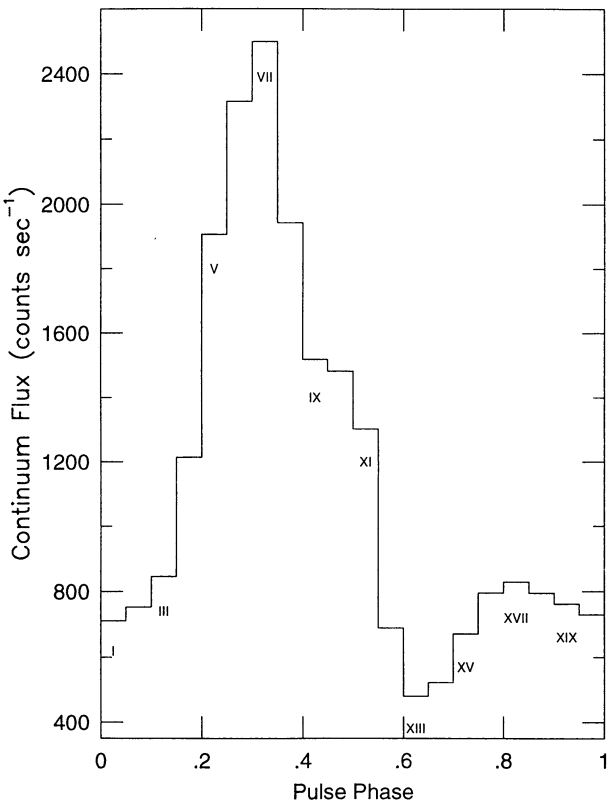

FIG. 1.—Phase-averaged pulse profile obtained from the observation from April 27 to May 4 in 1989. It was folded at the pulse period of 1.237757973 s determined by Deeter et al. (1991). The pulse phase is arbitrary.

3. DATA ANALYSIS

Pulse-phase dependent changes of the Her X-1 spectrum was observed by Pravdo et al. (1977b) and McCray et al. (1982). It has been understood that an anisotropic radiative transfer process in a strongly magnetized plasma is responsible for the spectral variation and an asymmetry in pulse shapes (Mészáros & Nagel 1985a, b; Kii et al. 1986; Leahy 1990). Thus, it is expected that a conventional power-law model with a high-energy cutoff plus an iron emission line is hard to describe the phase-dependent spectra, even though a phase-averaged spectrum of Her X-1 has been reproduced successfully with the model (see Kahabka 1987). In fact, we tried to fit the phase-dependent spectra with the above model in the energy range of *Ginga* observation. However, we could not obtain an acceptable fit with the above simple model, especially around the peak of main pulse, because of large deviations between the model and the observation.

3.1. *Method*

To concentrate on the reduction of iron line feature, we confine our analysis to the energy range of 3–11 keV, and we adopt a mathematical model which will be shown later. In the first step, we attempted to fit the phase-averaged spectrum with the conventional power-law plus iron emission line model, to form a reference continuum over the phase-resolved spectra, in which a Lorentzian function is adopted for a high-energy cutoff (see Makishima et al. 1990). The results are shown in

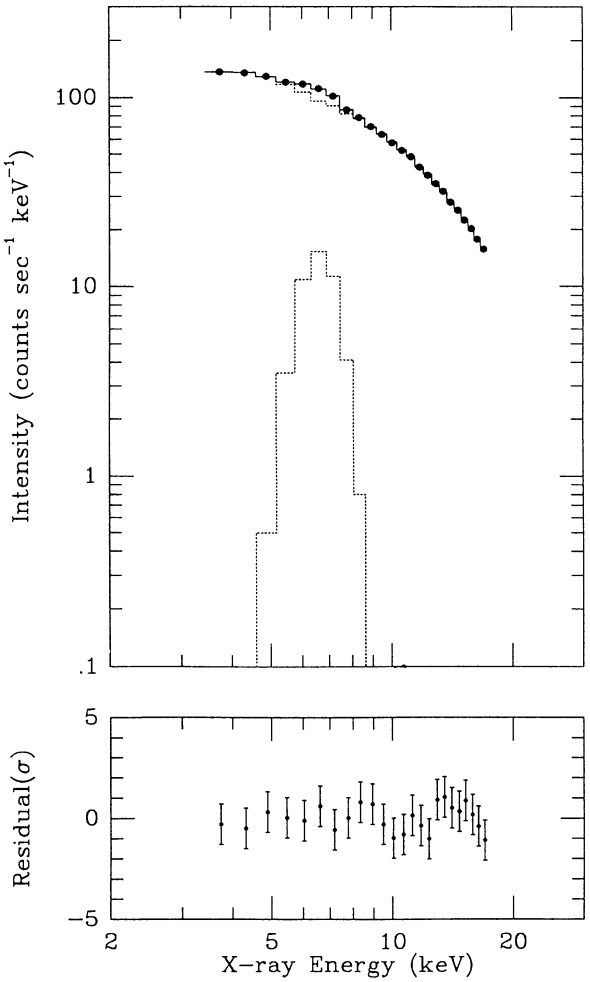

FIG. 2.—Model fit to the phase-averaged spectrum of Her X-1 observed from April 27 to May 4 in 1989. The dotted lines are each component of the best-fit model function (power-law with a high-energy cutoff for X-ray continuum and an iron emission line of Gaussian form), and the solid line is the sum. In the fitting, we adopted a form of Lorentzian function for a high-energy cutoff (Makishima et al. 1990). Lower panel of the figure indicates the residuals.

Figure 2 and Table 2. The best-fit parameters, i.e., the photon index, the line energy, and the line flux of 7.5×10^{-3} photons cm^{-2} s^{-1}, are consistent with that of a typical MAIN HIGH spectrum (see, e.g., Kahabka 1985; Mihara et al. 1991). We did not find a significant iron K-absorption edge at around 7–10 keV in the fitting and obtained only an upper limit of $N_H = 20.5$ cm^{-2} at the 90% confidence level, where cosmic abundance is assumed.

In order to extract an iron line profile, we divided each phase-resolved spectrum by the power-law continuum obtained from the above spectral fitting (see Day et al. 1993 for the details). This method was applied consistently to the data sets included to probe a line intensity variation over the various continuum X-ray levels. Figure 3 shows the obtained iron line profiles. The roman numerals in the figure corresponds to that of the pulse phase shown in Figure 1. We can see immediately that the continuum levels, before and after the line profile, change drastically at around the peak of main pulse, and those spectra cannot be explained with the simple power-law model. We assume here that continuum levels outside the line profile are smoothly connected in the phase-resolved spectra.

TABLE 3

BEST-FIT PARAMETERS FOR THE PHASE-RESOLVED IRON LINE[a]

Pulse Phase	I_{Fe}[b]	E_K[c]	EW[c]	χ^2_ν (8)
I	1.29 ± 0.21	6.59 ± 0.08	0.55 ± 0.28	1.36
II	1.11 ± 0.19	6.63 ± 0.09	0.44 ± 0.22	1.75
III	1.28 ± 0.22	6.63 ± 0.09	0.45 ± 0.21	0.68
IV	1.05 ± 0.21	6.62 ± 0.12	0.25 ± 0.11	0.73
V	0.86 ± 0.24	6.58 ± 0.22	0.13 ± 0.06	0.57
VI	1.00 ± 0.27	6.52 ± 0.21	0.14 ± 0.06	0.25
VII	0.94 ± 0.23	6.38 ± 0.17	0.13 ± 0.06	2.53
VIII	0.85 ± 0.22	6.40 ± 0.20	0.15 ± 0.07	0.41
IX	0.88 ± 0.21	6.34 ± 0.17	0.15 ± 0.06	0.41
X	0.58 ± 0.19	6.45 ± 0.25	0.11 ± 0.07	0.50
XI	0.69 ± 0.19	6.53 ± 0.19	0.16 ± 0.07	0.61
XII	0.82 ± 0.16	6.61 ± 0.11	0.35 ± 0.18	1.00
XIII	1.01 ± 0.16	6.59 ± 0.08	0.66 ± 0.40	1.92
XIV	1.13 ± 0.18	6.65 ± 0.07	0.67 ± 0.40	2.37
XV	1.05 ± 0.18	6.58 ± 0.08	0.48 ± 0.25	0.73
XVI	1.36 ± 0.22	6.58 ± 0.07	0.53 ± 0.26	0.73
XVII	1.05 ± 0.19	6.60 ± 0.10	0.38 ± 0.19	0.84
XVIII	0.97 ± 0.18	6.54 ± 0.11	0.37 ± 0.18	0.73
XIX	0.95 ± 0.18	6.58 ± 0.10	0.37 ± 0.19	1.48
XX	1.07 ± 0.19	6.52 ± 0.09	0.44 ± 0.22	1.71

[a] Quoted errors are 90% confidence level.
[b] I_{Fe} is the normalized line flux by the phase-averaged line flux.
[c] Iron line energy E_K and equivalent width EW are in units of keV.

3.2. *Spectral Fitting and Systematic Error*

Phase-resolved energy spectra of Her X-1 show large variations and there is no commonly accepted physical model which can fit the phase-resolved spectra satisfactorily. We have been chosen a model of a polynomial plus Gaussian to interpret the normalized spectra as follow;

$$I(E) = C_0 + C_1 E + C_2 E^2 + C_3 \exp\left[-\frac{(E - C_4)^2}{2C_5^2}\right], \quad (1)$$

where $C_{0,1,2}$ represent the coefficients of the normalized continuum and $C_{3,4,5}$ are the line parameters. The model fit has been carried out with the QDP/PLT software package (Tennant 1989). In the fitting, we fixed the line width as that of the phase averaged one except the low-state spectrum. Thus the spectral fitting has been performed with five free parameters using the above equation. In the case of the low-state spectrum, we found that the line width was 1.01 ± 0.31 keV

TABLE 2

THE FITTING RESULTS FOR THE PHASE-AVERAGED SPECTRUM

α (photon index)	I_{Fe} (photons s^{-1})	E_K (keV)	Γ[a] (keV)	EW (keV)	χ^2_ν (d.o.f.)
0.90 ± 0.01	29.6 ± 3.2	6.52 ± 0.07	1.08 ± 0.26	0.28 ± 0.03	0.61 (16)

[a] Intrinsic line width (FWHM).

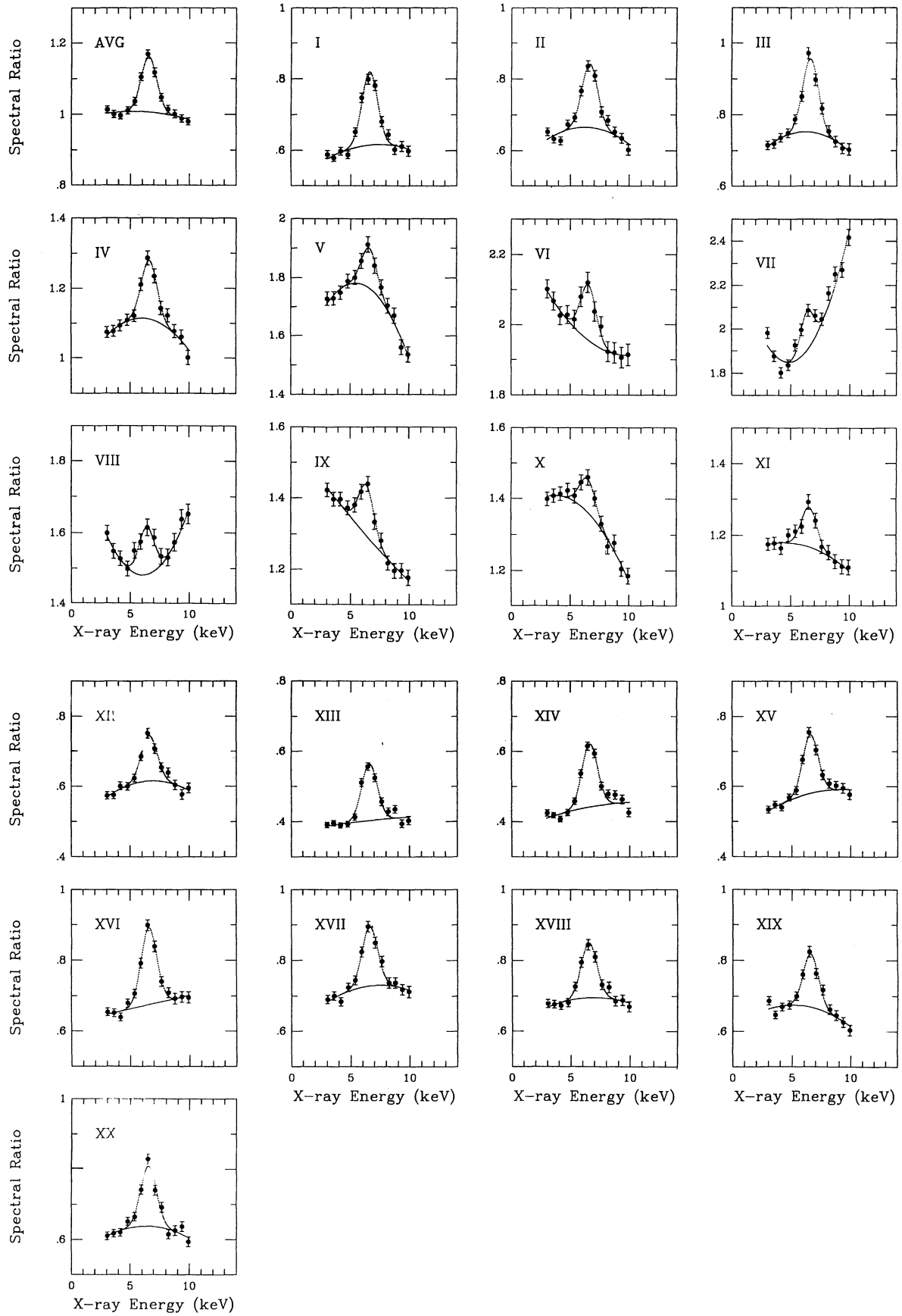

FIG. 3.—Iron line profiles over the 20 pulse-phase bins. Each spectrum is normalized by the model continuum of phase-averaged spectrum illustrated in Fig. 2 and Table 2. The roman numerals in the figure corresponds to that of the pulse phase shown in Fig. 1.

TABLE 4

THE LINE PARAMETERS FOR THE VARIOUS CONTINUUM LEVELS[a]

I_0[b]	Ψ_{35}[c]	Φ_{orb}[c]	I_{Fe}	E_K	EW	χ^2_ν (8)
1.09	0.04	0.22	1.09 ± 0.21	6.63 ± 0.12	0.26 ± 0.09	0.49
1.15	0.12	0.91	0.99 ± 0.18	6.43 ± 0.11	0.23 ± 0.07	0.44
1.07	0.15	0.57	1.09 ± 0.19	6.53 ± 0.09	0.27 ± 0.09	0.74
0.77	0.20	0.62	0.85 ± 0.15	6.64 ± 0.09	0.34 ± 0.11	1.13
0.51	0.23	0.20	0.69 ± 0.12	6.55 ± 0.08	0.36 ± 0.13	0.20
0.28	0.63	0.35	0.43 ± 0.08	6.60 ± 0.12	0.37 ± 0.21	0.92
0.23	0.68	0.48	0.43 ± 0.07	6.60 ± 0.13	0.47 ± 0.30	1.80
0.04[d]	0.56–0.60[e]	0.41–0.50[e]	0.12 ± 0.02	6.51 ± 0.03	1.02 ± 0.65	0.94
0.008[f]	0.12	0.93–1.02	≤ 0.02	...	≤ 0.44	1.84

[a] Designation and units of the parameters are the same as in Table 3.
[b] The observed continuum flux in the range of 7.1–37 keV, which is normalized by that of the phase-averaged spectrum.
[c] The epoch from Deeter et al. 1991.
[d] The low-state spectrum adopted from Mihara et al. 1991. The calculated line width is 1.01 ± 0.31 keV FWHM.
[e] The 35 day and orbital phases are from Mihara et al. 1991.
[f] The eclipse spectrum adopted from Choi et al. 1994a.

(FWHM). The dotted lines of Figure 3 and Figures 6*a* and 6*b* below represent the best-fit model, respectively. The fitting results are summarized in Table 3 for the pulse phase-resolved spectra and in Table 4 for the spectra taken from different intensity states of Her X-1, respectively. The acceptable reduced chi-square values explain that the above model describes the observed data relatively well.

We cross-checked how the selection of the continuum spectrum affects the iron line parameters by taking the model of the low-state spectrum presented by Mihara et al. (1991) as an example. Figure 4 shows the two diffent continuum models obtained, in which filled circles and dotted line, respectively, correspond to the result of Mihara et al. and the present work. With these models, the systematic error, which occurs when we calculate the line flux using the continuum X-ray models, is estimated to be about 8%. This value is within the statistical error attached in Table 3 and Table 4.

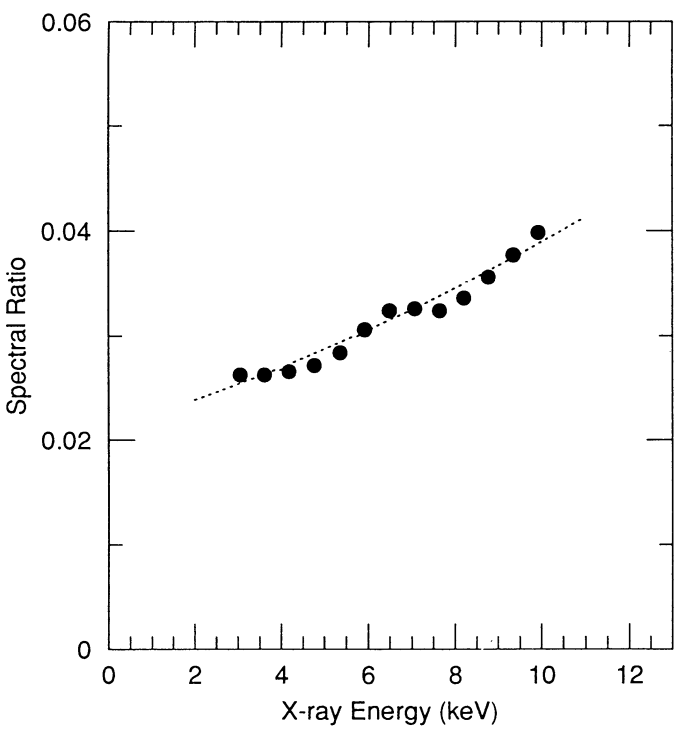

FIG. 4.—Comparison of the model continua obtained from two different methods for the low-state spectrum. The dotted line in the figure indicates the calculated spectrum using eq. (1), and the filled circles are sum of the two scattered components suggested by Mihara et al. (1991). Both of the above models were normalized by the model continuum of the phase-averaged spectrum.

4. RESULTS

4.1. *Pulse-phase Dependence*

We obtain the line parameters to the phase-resolved spectra shown in Table 3. The weighted average of the normalized line flux and the center energy are 1.00 ± 0.20 which corresponding to 29.6 ± 6.0 photons s^{-1} (see Table 2) and 6.55 ± 0.13 keV, respectively. These values are in good agreeement with the results of the phase-averaged spectrum presented in Table 2. Figure 5 displays the best-fit parameter values of the line flux and equivalent width, as well as the continuum X-ray flux against the pulse phase. The line flux is derived by integrating the Gaussian profile mentioned in the previous section. From this and the results of Table 3, we find the following facts; (1) the line flux changes from $(4.3 \pm 1.9) \times 10^{-3}$ to $(1.0 \pm 0.3) \times 10^{-2}$ photons cm^{-2} s^{-1} (the average is 7.5×10^{-3} photons cm^{-2} s^{-1}) through one cycle of the pulse period, (2) the equivalent width varies from 0.11 to 0.67 keV, and the variation shows an inverse proportionality to that of the continuum flux, (3) there is a phase difference of $\Delta\psi \approx 0.15$ between the pulse peak and the line flux minimum.

4.2. *Dependence on the Orbital Phase and on the 35 day Cycle*

Further line flux variations have been investigated with the spectra taken at the various intensity level of Her X-1. All those spectra were normalized by the continuum model of phase-averaged spectrum described in § 3.1, and the spectral fitting carried out with equation (1). Figures 6*a* and 6*b* show the examples. The calculated line flux and equivalent width are plotted against the continuum intensity of 7.1–37 keV in Figures 6*c* and 6*d*, respectively. The dependence on orbital phase is shown in the left panel of Figure 7, and the 35 day cycle dependence is in the right panel. From the results shown

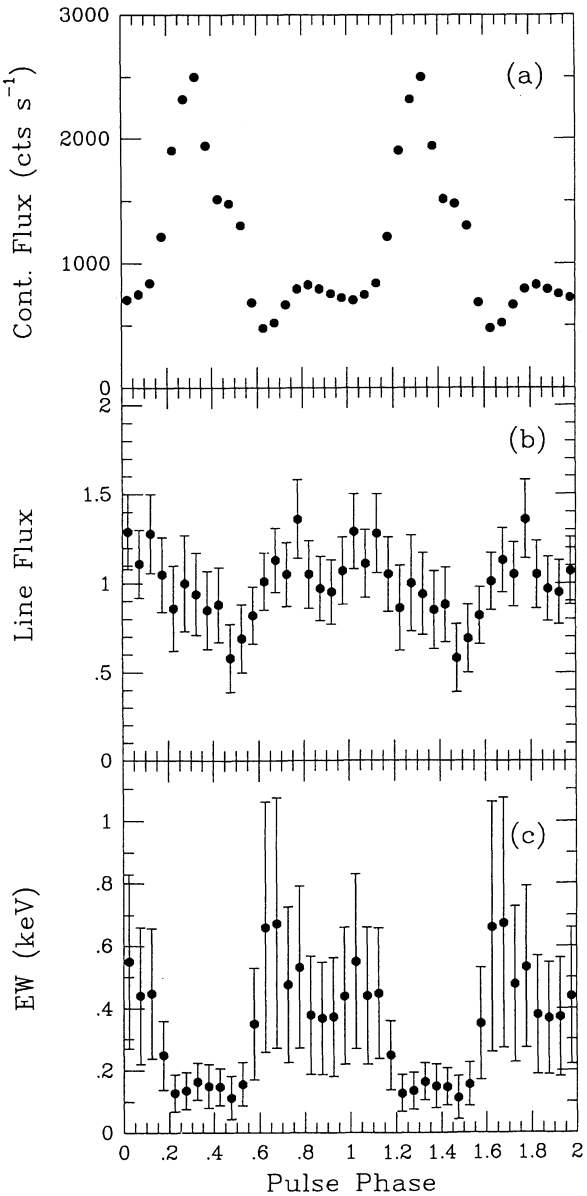

FIG. 5.—Plot of the best-fit parameters obtained from the fits for the pulse-dependent spectra against the pulse phase: (*a*) observed continuum flux (counts s^{-1}) in the energy range 1.7–37 keV, (*b*) Normalized iron line flux derived by integrating the Gaussian model of eq. (1), (*c*) the equivalent width of the iron line in units of keV.

in Figures 6 and 7 and summarized in Table 4, we see the following properties:

1. There is a correlation between the line flux and continuum flux of 7.1–37 keV. However, the relation does not appear to be linear (Fig. 6*c*). This is apparent from the fact that when the continuum flux of the low-state decreases to ~4% of the flux of the MAIN HIGH state, the iron line flux shows a decrease of ~10% (Table 4).

2. The line flux of the MAIN HIGH state does not depend significantly on the orbital phase of $\Phi_{orb} = 0.2$–0.9, while the flux is almost invisible during the eclipse phase. The upper limit of the line flux of eclipse is about 2% of the MAIN HIGH average.

3. The pattern of iron line flux modulation along the 35 day cycle is very similar to that of continuum flux variation. The equivalent width varies from 0.23 to 1.02 keV depending on the characteristic intensity state of Her X-1.

5. DISCUSSION

The fluorescent iron K line, which is a useful tool for investigating the matter distribution in binary X-ray pulsars, can arise from various regions illuminated by the continuum X-rays from the central source. The measurable line parameters, i.e., the line center energy, the line width, and the equivalent width provide valuable information on the physical characteristics of the line emitting gases, and also constrain the possible sites of the line emission.

Several regions introduced in § 1 can be considered as the line reprocessing site of Her X-1. The observed equivalent width of ~0.2 keV during the MAIN HIGH state requires a matter distribution having a relatively large solid angle ($\Omega/4\pi$) ~0.2, as seen from the neutron star (Inoue 1985; Makishima 1986). The line pulsations discovered in § 4.1 suggest a localized emission site. Therefore, with these facts, we can derive a conclusion reasonably that the companion star atmosphere and the outer edge of the accretion disk of Her X-1 cannot be responsible for the line emission of 7.5×10^{-3} photons cm^{-2} s^{-1} during the MAIN HIGH state (see Basko 1978 and also discussion on the possible line emission site of Her X-1 by Choi et al. 1994b). No orbital phase dependence of the line flux shown in the left panel of Figure 7 excludes also the companion star origin. If we assume that the line emission originates from an accretion disk of the neutron star neighborhood, the line pulsations constrain the emission region as follow;

$$d < \frac{cP_s}{2 \cos i} \sim 10^{10} \text{ cm} \qquad (2)$$

where d, c, P_s, and i are the extent of reprocessing site on the disk, the light velocity, the pulse period of Her X-1, and the inclination angle of an accretion disk with respect to an observer, respectively. This limit is an order of smaller than that of an accretion disk corona (~10^{11} cm). It appears plausible that the Alfvén surface at distance $r \approx 3 \times 10^8$ cm from the neutron star is responsible for the line emission. If then, this region should have an appropriate solid angle mentioned above with respect to the neutron star. The equivalent width during the pulse period varies 0.11 to 0.67 keV, which shows inversely proportional to that the continuum flux (Fig. 5*c*). This may imply a dramatic matter distribution around the neutron star. The iron line flux changes by about 30% from $(4.3 \pm 1.9) \times 10^{-3}$ to $(1.0 \pm 0.3) \times 10^{-2}$ photons cm^{-2} s^{-1} about the phase-averaged value of 7.5×10^{-3} photons cm^{-2} s^{-1} through one cycle of the pulse period, while the continuum flux varies by a factor of 2 about an pulse-averaged mean value. Hence, the equivalent width profile seems to be established mainly by beaming effects of the neutron star rather than the asymmetry of the matter distribution.

It is interesting to note that an intense soft X-ray emission, interpreted as a consequence of the reprocessing of hard X-rays by the matter near the Alfvén surface, has been observed from Her X-1 at energies below 1 keV (Shulman et al. 1975; Catura & Acton 1975; McCray et al. 1982; Mavromatakis 1993). McCray et al. (1982) found a pulse phase difference ($\Delta\psi \approx 0.68$) between hard (1–5 keV) and soft X-ray ($\lesssim 0.85$ keV) peaks, and they interpreted the soft X-rays as a consequence of the reprocessing of the hard X-rays by an inner accretion disk. The iron

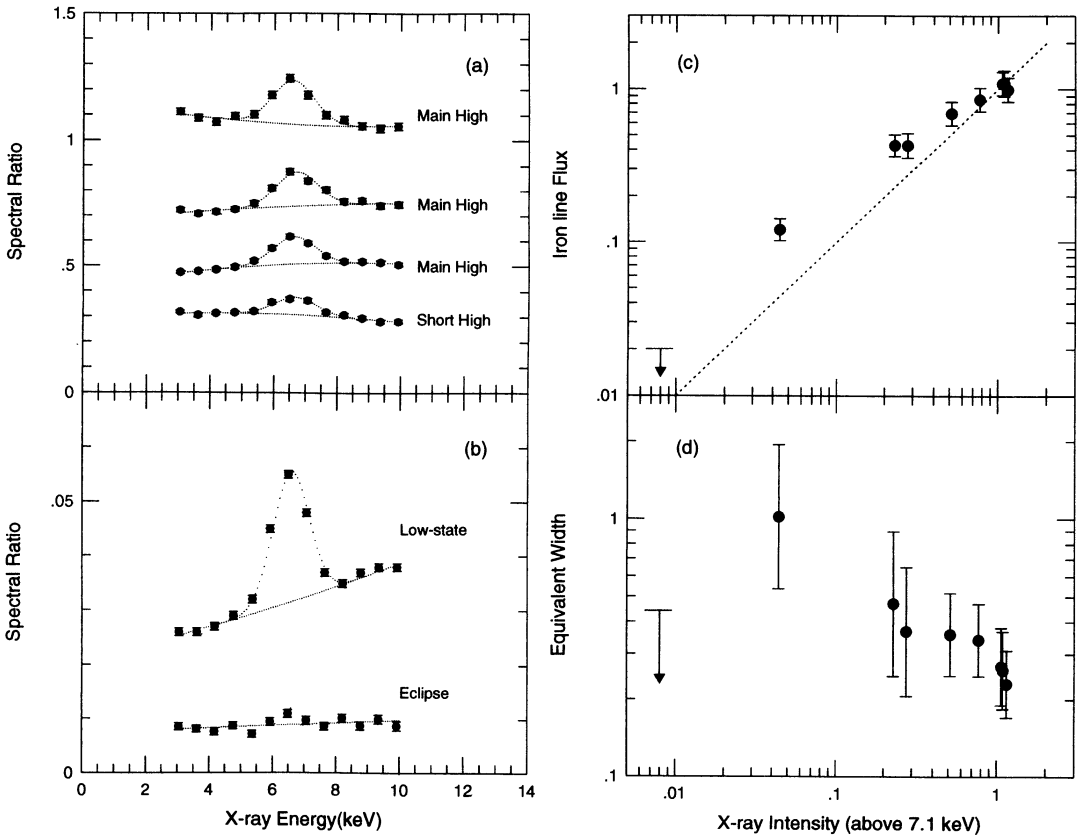

FIG. 6.—Iron line flux and equivalent width over the various continuum X-ray levels. The spectra included in (*a*) and (*b*) were all normalized by the model continuum of the phase-averaged spectrum shown in Fig. 2, and the spectral fitting was carried out using eq. (1). The calculated line flux and the equivalent width are plotted against the observed continuum flux (in the energy range 7.1–3.7 keV) in (*c*) and (*d*), respectively. Dashed line in (*c*) represents an assumed linear correlation between the line flux and the continuum flux.

line flux variations over the pulse phase obtained in § 4.1 are consistent with the soft X-ray behavior presented by McCray et al. (1982): i.e., the phase difference of $\Delta\psi \approx 0.15$ between the pulse peak and the flux minimum of the iron line and the variation pattern of the iron line. From these facts we conclude that the reprocessed iron line and the soft X-ray emission originate from the same place as predicted by previous works. We recognized that there is no significant iron K-absorption feature from the fitting of phase-averaged spectrum described in § 3. This fact may imply that the direct beam is not obscured by the line reprocessing matter or the contribution of the obscuring matter is very small. For the phase difference between the pulse peak and the flux minimum of the iron line, we do not yet have a clear answer. It may be due to misalignment of the rotation axis of the neutron star and the symmetry axis of the Alfvén surface material as discussed by McCray et al. (1982).

We have observed a broadened iron line (the intrinsic line width 1.08 ± 0.26 keV at FWHM), which has a line center energy of 6.52 ± 0.07 keV, from the phase-averaged spectrum of MAIN HIGH (see Table 2). In terms of the line broadening, two possibilities, when we consider the expected line width (Pozdnyakov, Sobol, & Sunyaev 1979; Kallman & White 1989, and references therein), could be suggested reasonably such as a mixture of multiple line originate from different degree of ionization state of iron and Comptonization by hot and optically thick plasma. Unfortunately, our data do not have enough energy resolution to distinguish which mechanism is appropriate for the broadening line. The line center energy which is in between that of cold matter and the highly ionized matter, may indicate a mixture of lines.

We now discuss the line flux behavior along the 35 day cycle. Figure 6*c* shows that the decrease of the line flux is correlate with that of continuum X-ray of the energy range 7.1–37 keV. Moreover, the line flux modulation shown in Figure 7 (*right panel*) is almost similar to the behavior of the continuum X-ray. According to Deeter et al. (1976), an optical flux variation of HZ Her due to X-ray heating of the companion star atmosphere is stable during the 35 day period. This implies that the intrinsic luminosity of Her X-1 does not change, even though pulsed X-rays are invisible during the low-intensity state of Her X-1. Hence the line flux variation cannot be explained with a change of the intrinsic X-ray intensity of Her X-1. In § 4.2 we revealed the correlation between the line flux and the continuum flux of 7.1–37 keV is not linear. As an example, when the continuum flux of the SHORT HIGH state decreases to ~30% of the flux of the MAIN HIGH, the iron line flux shows a decrease of ~40% (see Table 4 and the right panel of Fig. 7). The equivalent width change from 0.23 to 1.02 keV shown in Figure 6*d* and in the right panel of Figure 7 are consistent with this. The difference could be due to line flux contributed from an additional site or to partial covering of the line emission site. It is noteworthy that the soft X-ray flux observed during the SHORT HIGH state (Mavromatakis

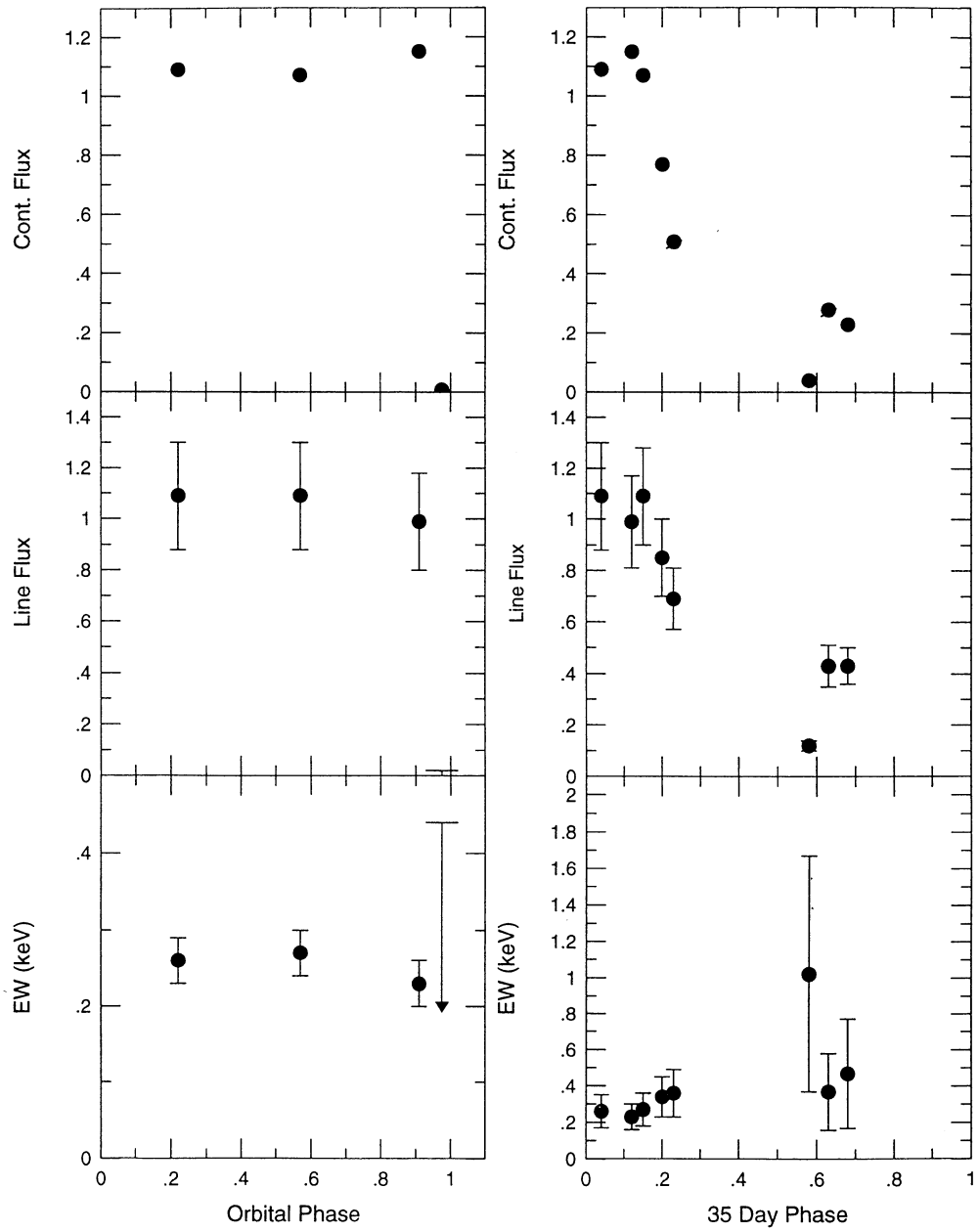

FIG. 7.—Variation of the continuum flux and the line flux over the orbital phase (*left panel*), and along the 35 day cycle (*right panel*). In the figures, the continuum flux and the iron flux are respectively normalized by that of the phase-averaged spectrum.

1993) corresponds to ~30% of the MAIN HIGH flux (McCray et al. 1982) in the same energy range of 0.1–0.7 keV. Therefore, it may be reasonable that an additional line flux is responsible for the equivalent width change. During the low-state of Her X-1, we cannot see the pulsed direct beam but see only scattered flux (see, e.g., Mihara et al. 1991). If we assume an highly ionized accretion disk corona is responsible for the scattering, the line flux generated from the Alfvén surface should suffer from the same amount of scattering. With this picture and electron column density of the accretion disk corona suggested by Choi et al. (1994b), we calculate the observed line flux of the low-state is to be $\sim 4 \times 10^{-4}$ photons cm^{-2} s^{-1}. This corresponds to half of the observed line flux ($\sim 9 \times 10^{-4}$ photons cm^{-2} s^{-1}). Thus an additional amount of $\sim 5 \times 10^{-4}$ photons cm^{-2} s^{-1} should be emitted from other places. The required amount is an order of smaller than that the MAIN HIGH flux. The outer edge of the accretion disk discussed by previous authors may be the additional emission site.

We would like to express our gratitude to Professor A. C. Fabian for careful reading and helpful comments on the manuscript. We are also indebted to T. Mihara for providing us the low-state spectrum. C. S. C. wishes to thank K. Yoshida for help in using the *Ginga* software. He is grateful to Japan Society for Promotion of Science for a research fellowship and also to Korea Science and Engineering Foundation for supporting his visit.

REFERENCES

Bai, T. 1980a, ApJ, 239, 328
———. 1980b, ApJ, 239, 999
Basko, M. M. 1978, ApJ, 223, 268
———. 1980, A&A, 87, 330
Basko, M. M., & Sunyaev, R. A. 1976, Soviet Astron., 20, 537
Catura, R. C., & Acton, L. W. 1975, ApJ, 202, L5
Choi, C. S., Dotani, T., Nagase, F., Makino, F., Deeter, J. E., & Min, K. W. 1994a, ApJ, 427, 400
Choi, C. S., Nagase, F., Makino, F., Dotani, T., & Min, K. W. 1994b, ApJ, 422, 799
Day, C. S. R., Nagase, F., Asai, K., & Takeshima, T. 1993, ApJ, 408, 657
Deeter, J. E., Boynton, P. E., Miyamoto, S., Kitamoto, S., Nagase, F., & Kawai, N. 1991, ApJ, 383, 324
Deeter, J. E., Crosa, L., Gerend, D., & Boynton, P. E. 1976, ApJ, 206, 861
Deeter, J. E., Scott, D. M., Boynton, P. E., Miyamoto, S., Kitamoto, S., Takahama, S., & Nagase, F. 1994, ApJ, in press
Ghosh, P., & Lamb, F. K. 1979, ApJ, 232, 259
Giacconi, R., Gursky, H., Kellogg, E., Levinson, R., Schreier, E., & Tananbaum, H. 1973, ApJ, 184, 227
Gottwald, M., & White, N. E. 1990, in Iron Line Diagnostics, ed. A. Treves, G. C. Perola, & L. Stellar (Berlin: Springer), 134
Hirano, T., Hayakawa, S., Nagase, F., Masai, K., & Mitsuda, K. 1987, PASJ, 39, 619
Inoue, H. 1985, Space Sci. Rev., 40, 317
Kahabka, P. 1987, Ph.D. thesis, Univ. München
Kahabka, P., Ögelman, H., Pietsch, W., Trümper, J., & Voges, W. 1985, Space Sci. Rev., 40, 355
Kallman, T., & White, N. E. 1989, ApJ, 341, 955
Kii, T., Hayakawa, S., Nagase, F., Ikegami, T., & Kawai, N. 1986, PASJ, 38, 751
Leahy, D. A. 1990, MNRAS, 242, 188
Leahy, D. A., & Matsuoka, M. 1990, ApJ, 355, 627
Leahy, D. A., Matsuoka, M., Kawai, N., & Makino, F. 1989, MNRAS, 237, 269
Makino, F., & Astro-C team. 1987, Astrophys. Lett., 25, 223
Makishima, K. 1986, in The Physics of Accretion onto Compact Objects, ed. K. O. Mason, M. G. Watson, & N. E. White (New York: Springer), 249
Makishima, K., et al. 1990, PASJ, 42, 295
Mavromatakis, F. 1993, A&A, 273, 147
McCray, R. A., Shull, J. M., Boynton, P. E., Deeter, J. E., Holt, S. S., & White, N. E. 1982, ApJ, 262, 301
Mészáros, P., & Nagel, W. 1985a, ApJ, 298, 147
———. 1985b, ApJ, 299, 138
Mihara, T., Ohashi, T., Makishima, K., Nagase, F., Kitamoto, S., & Koyama, K. 1991, PASJ, 43, 501
Nagase, F. 1989, PASJ, 41, 1
Nagase, F., Hayakawa, S., Sato, N., Masai, K., & Inoue, H. 1986, PASJ, 38, 547
Ohashi, T., et al. 1984a, PASJ, 36, 719
———. 1984b, PASJ, 36, 699
Pozdnyakov, L. A., Sobol, I. M., & Sunyaev, R. A. 1979, A&A, 75, 214
Pravdo, S. H., Becker, R. H., Boldt, E. A., Holt, S. S., Serlemitsos, P. J., & Swank, J. H. 1977a, ApJ, 215, L61
Pravdo, S. H., Boldt, E. A., Holt, S. S., Rothschild, R. E., & Serlemitsos, P. J. 1978, ApJ, 225, L53
Pravdo, S. H., Boldt, E. A., Holt, S. S., & Serlemitsos, P. J. 1977b, ApJ, 216, L23
Sato, N., et al. 1986, PASJ, 38, 731
Shulman, S., Friedman, H., Fritz, G., Henry, R. C., & Yentis, D. J. 1975, ApJ, 199, L101
Tananbaum, H., Gursky, H., Kellogg, E. M., Levinson, R., Schreier, E., & Giacconi, R. 1972, ApJ, 174, L143
Tennant, A. F. 1989, The QDP/PLT User's Guide (Huntsville: NASA/MSFC)
Turner, M. J. L., et al. 1989, PASJ, 41, 345
White, N. E., et al. 1986, MNRAS, 218, 129
White, N. E., Swank, J. H., & Holt, S. S. 1983, ApJ, 270, 711